Bull Volcanol (1997) 58:566–579

ORIGINAL PAPER

M. J. Wooster · D. A. Rothery

Thermal monitoring of Lascar Volcano, Chile, using infrared data from the along-track scanning radiometer: a 1992–1995 time series

Received: 1 October 1996 / Accepted: 13 January 1997

Abstract Lascar Volcano (22°22'S, 67°44'W) is the most active volcano of the central Andes of northern Chile. Activity since 1984 has been characterised by periods of lava dome growth and decay within the active crater, punctuated by explosive eruptions. We present herein a technique for monitoring the high-temperature activity within the active crater using frequent measurements of emitted shortwave infrared (SWIR) radiation made by the spaceborne along-track scanning radiometer (ATSR). The ATSR is an instrument of low spatial resolution (pixels 1 km across) that shares certain characteristics with the MODIS instrument, planned for use as a volcano monitoring tool in the NASA EOS Volcanology Project. We present a comprehensive time series of over 60 cloud- and plume-free nighttime ATSR observations for 1992–1995, a period during which Lascar experienced its largest historical eruption. Variations in short wavelength infrared flux relate directly to changes in high-temperature surfaces within the active crater. From these data, interpretations can be made that supplement published field reports and that can document the presence and status of the lava dome during periods where direct, ground-based, observations are lacking. Our data agree with less frequent information collected from sensors with high spatial resolution, such as the Landsat thematic mapper (Oppenheimer et al. 1993) and are consistent with field observations and models that relate subsidence of the dome to subsequent explosive eruptions (Matthews et al., 1997). Most obviously, Lascar's major April 1993 eruption follows a period in which the magnitude of emitted shortwave infrared radiation fell by 90%. At this time subsidence of the 1991–1992 lava dome was reported by field observers and this subsidence is believed to have impeded the escape of hot volatiles and ultimately triggered the eruption (Smithsonian Institution 1993a). Extrapolating beyond the period for which field observations of the summit are available, our data show that the vulcanian eruption of 20 July 1995 occurred after a period of gradual increase in short wavelength infrared flux throughout 1994 and a more rapid flux decline during 1995. We attribute this additional, otherwise undocumented, cycle of increasing and decreasing SWIR radiance as most likely representing variations in degassing through fumaroles contained within the summit crater. Alternatively, it may reflect a cycle of dome growth and decay. The explosive eruption of 17 December 1993 appears to have followed a similar, but shorter, variation in SWIR flux, and we conclude that large explosive eruptions are more likely when the 1.6-μm signal has fallen from a high to a low level. The ATSR instrument offers low-cost data at high temporal resolution. Despite the low spatial detail of the measurements, ATSR-type instruments can provide data that relate directly to the status of Lascar's lava dome and other high-temperature surfaces. We suggest that such data can therefore assist with predictions of eruptive behaviour, deduced from application of physical models of lava dome development at this and similar volcanoes.

Key words Lascar Volcano · ATSR (Along Track Scanning Radiometer) · Remote sensing · Infrared

Editorial responsibility: J. Fink

M. J. Wooster · D. A. Rothery (✉)
Department of Earth Sciences, The Open University,
Milton Keynes, UK
Fax: +01908 655151
e-mail: m.j.wooster@open.ac.uk, d.a.rothery@open.ac.uk

M. J. Wooster
The Natural Resources Institute, University of Greenwich,
Chatham, Kent, UK

Introduction

Lascar is the most active volcano of the central Andes of northern Chile (Oppenheimer et al. 1993). The vol-

cano is located at 22°22'S, 67°44'W, 34 km from the village of Toconao, and possesses a single active crater at 5450 m altitude. Lascar's activity is characterised by continuous fumarolic degassing, punctuated by occasional vulcanian explosive eruptions. The majority of these eruptions are small and create ash columns extending up to a few kilometres above the summit. On a number of occasions, however, larger eruptions have taken place. Most notable are the events of 16 September 1986, 20 February 1990 and 18–20 April 1993, when eruption columns rose 10, 14 and 20 km, respectively, above Lascar's summit. Each led to ashfall many hundreds of kilometres away from the volcano. The September 1986 eruption was the first obvious sign of magmatic activity at Lascar for over 20 years, though retrospective study of Landsat thematic mapper data reveals the presence of a hot feature (now accepted to have been a lava dome) within the active crater since at least December 1984 (Francis and Rothery 1987; Rothery et al. 1988; Glaze et al. 1989a, b). The April 1993 eruption is the largest thus far, and caused ash to fall on Buenos Aires, 1500 km downwind. The same event also produced pyroclastic flows that travelled 7.5 km down the slopes of the volcanic complex.

Lascar's eruptive activity was first related to the growth and deflation of a lava dome by Oppenheimer et al. (1993). However, being remote, Lascar is not routinely monitored. Infrequent visits to the summit and temporary seismographic monitoring comprise the majority of observations. In addition to these studies, occasional reconnaissance flights by the Chilean Air Force have provided a useful photographic record of summit conditions. (The reader is referred to Matthews et al., 1997, for further general discussion of Lascar Volcano.)

Previous satellite observations of Lascar Volcano

Satellite remote sensing studies of Lascar's active crater were first made using data from the Landsat thematic mapper (TM) instrument (Francis and Rothery 1987; Rothery et al. 1988; Glaze et al. 1989a). From these 30- × 30-m shortwave infrared (SWIR) measurements at 1.6 μm (TM band 5) and 2.5 μm (TM band 7) the investigators indicated the presence of a high-temperature thermal anomaly within the active crater of the volcano. Use of multi-temporal TM data allowed the evolution of SWIR radiance to be studied and related to changes in summit activity. Oppenheimer et al. (1993) used TM images from 15 dates to document the summit activity between 1984 and 1992, later supplementing this with a February 1993 measurement (Smithsonian Institution 1993a). Figure 1 includes TM 1.6-μm radiance data from Oppenheimer et al.'s time series, along with ATSR data that are discussed later. The TM data indicate that the levels of thermally anomalous 1.6-μm radiance fell dramatically prior to the major eruptions of September 1986 and April 1993, which leads to the conclusion that major changes in surface temperature preceded both these events. It is also possible that a fall in SWIR radiance occurred prior to the February 1990 eruption, but this cannot be confirmed because of a long data gap between November 1987 and October 1989.

In March 1990, thermal measurements were made in the field to supplement the TM data. These measurements indicated that the broad area of the dome surface had a temperature of 100–200 °C, but that smaller areas, believed to be heated by the escape of magmatic gas, had temperatures greater than 900 °C (Oppen-

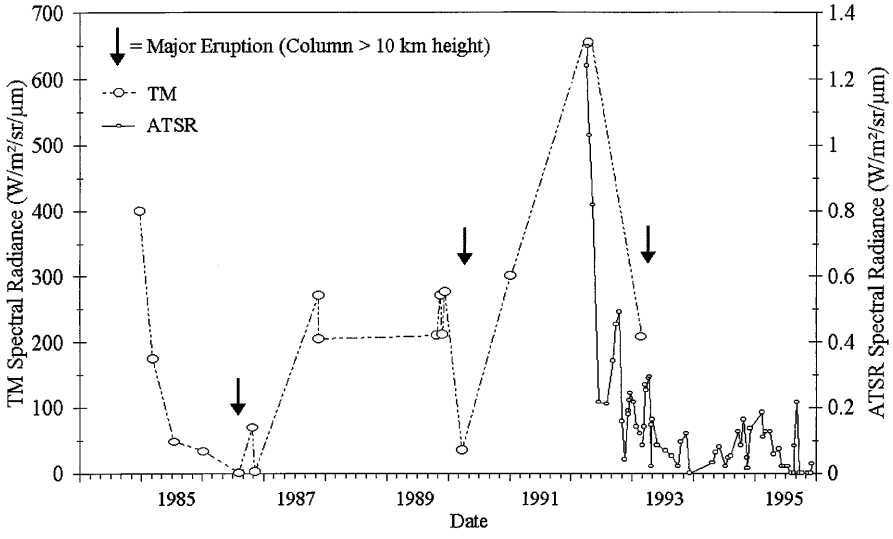

Fig. 1 Total spectral radiance of thermal origin recorded in the 1.6-μm channels of the Landsat thematic mapper (TM) and along-track scanning radiometer (ATSR) sensors. The vertical axes are scaled to equalise the peak values of radiance recorded by each sensor. A notable decrease in TM 1.6 μm radiance is evident prior to the September 1986 and April 1993 major explosive eruptions. This decrease is also mirrored by the ATSR 1.6-μm data recorded prior to the April 1993 event. The 2-year TM data gap between 1987 and 1989 precludes the detection of any such decrease in TM 1.6-μm radiance prior to the February 1990 eruption (TM data taken from Oppenheimer et al. 1993 and Smithsonian Institution 1993a)

heimer et al. 1993). We postulate that any restriction in degassing may be expected to lead to cooling of these high-temperature surfaces and thus to a fall in emitted SWIR radiance. Deflation of the lava dome has been proposed as a mechanism that would restrict the escape of hot gases through the bulk of the dome (Oppenheimer et al. 1993) and, on this basis, Oppenheimer et al. (1993) concluded that Lascar experienced at least two cycles of lava dome extrusion and decay between 1984 and 1993, these being separated by the large explosive eruption of September 1986.

Linking remotely sensed observations and pre-eruptive change

The information derived from Landsat TM has contributed to the development of a physical model that relates the extrusion and decay of the lava dome to the magmatic gas parameters that are believed to control the volcano's explosive activity (Matthews et al., 1997). The model treats the magma within the eruptive conduit as a permeable magmatic foam. As degassing proceeds, the magma vesicularity is reduced and the magma becomes less permeable to the flow of gas. Degassing also reduces the total volume occupied by the magma, resulting in subsidence of the lava dome surface. This may further restrict degassing by blocking the fracture system through which the gas permeates. Fumaroles distant from the collapse zone may allow the continued escape of some gas, but if this is not sufficient to relieve the increasing pressure an explosive eruption may occur. Matthews et al. (1997) have calculated that complete degassing of the foam layer would take between 13 and 330 days depending on the porosity of the magma.

The Matthews et al. model provides a physical mechanism that can be used to link observed decreases in SWIR radiance, caused by decreases in magmatic gas flux, to eruptive events driven by rising internal pressure. We conclude that the decreases in SWIR radiance, shown in the TM data of Fig. 1, indicate the onset of pressure buildup that led to major explosive eruptions many months after the SWIR radiance began to fall.

This finding suggests that SWIR radiance monitoring could be a valuable means for detecting certain pre-eruptive changes at Lascar. Unfortunately, routine monitoring of the volcano using Landsat TM data is made impractical by high data costs, limited data availability and long delivery times (Rothery et al. 1992). The TM data cost upwards of US $2000 per scene and, though Landsat passes over Lascar once by day and once by night every 16 days, cloud sometimes obscures the volcano's summit. Additionally, the collection of nighttime data, the most valuable for quantitative analysis, is not routine and must be scheduled well in advance of the satellite overpass. These limitations restrict the 1984–1993 TM time series shown in Fig. 1 to 16 scenes, the majority of which are daytime data (see Oppenheimer et al. 1993 for a full discussion). Furthermore, the scenes are not evenly distributed over this period. The 2-year gap between November 1987 and October 1989, when no suitable data are available, has already been noted. To be more appropriate for time-series monitoring, data must be inexpensive and acquired at a temporal frequency closer to the 13-day minimum degassing time scale calculated by Matthews et al. (1997). The purpose of our study was to determine whether potentially volcanologically useful SWIR radiance information can be provided by data whose spatial resolution is low, but which satisfy the desired characteristics of low-cost and high-temporal frequency.

New satellite observations of Lascar at low-spatial and high-temporal resolution

The spatial resolution and temporal frequency of spaceborne remote sensing devices are, in practice, inversely related (Lillesand and Kiefer 1991). It is thus possible to improve temporal coverage by taking measurements at a lower spatial resolution. A new generation of low-spatial-resolution satellite sensors is operating with an increased number of spectral channels, including some in the shortwave infrared (Holdaway 1993; Asrar and Jon Dokken 1993). Data from these instruments offer the possibility of volcanic SWIR monitoring at high temporal resolution.

We have used data from the along-track scanning radiometer (ATSR), which shares certain spatial resolution and waveband characteristics with the MODIS sensor, due to be launched by NASA on the EOS-AM platform in 1998. Shortwave and thermal infrared data from MODIS will be an important component of the EOS Volcanology Project (Mouginis-Mark et al. 1991a) and studies using ATSR may provide an indication of the capabilities MODIS offers for certain volcanological applications.

The along-track scanning radiometer

Background

The first along-track scanning radiometer (ATSR-1) was launched on the first European Remote Sensing Satellite (ERS-1) on 17 July 1991. The second-generation instrument (ATSR-2) was launched on ERS-2 on 21 April, 1995. Delderfield et al. (1985) give a good introduction to the special capabilities of the ATSR instrument, and only a brief outline is provided herein.

The ATSR was designed to record global sea-surface temperatures by making measurements of ocean-emitted radiance in three thermal infrared wavebands and through two different atmospheric path lengths (Fig. 2). The ATSR's three longer wavelength infrared

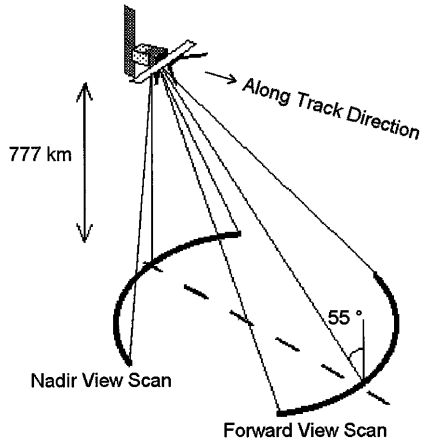

Fig. 2 The viewing geometry of the ATSR sensor, mounted onboard the orbiting ERS spacecraft. Every 150 ms the sensor makes two scans of the Earth's surface. The nadir-view scan views at zenith angles 0–22°, the forward-view scan views at zenith angles 53–55°. As the satellite moves along the orbit track each ground location is imaged in both the nadir and forward views

channels are centred on the same wavelengths (3.7, 11 and 12 μm) as those of the more familiar advanced very high resolution radiometer (AVHRR), which has previously been used to study the characteristics of volcanic ash plumes (e.g. Matson 1984; Prata 1989; Holasek and Rose 1991; Wen and Rose 1994) and lava flows (Mouginis-Mark et al. 1991b; Harris and Rothery 1995; Harris et al. 1995). The spatial resolution of the ATSR measurements is also similar to that of the AVHRR, approximating 1 km^2 in the nadir view (on which we concentrate in this study) and 4.5 km^2 in the forward view. However, ATSR differs significantly from AVHRR in that it possesses an additional short wavelength infrared channel, centred at 1.6 μm. This waveband was included to assist daytime cloud detection but, fortuitously, it enables monitoring of thermally emitted SWIR radiation at a high-temporal frequency, albeit at much reduced levels of spatial detail when compared with band 5 of Landsat TM (30 m).

An indication of the spatial resolution of ATSR's measurements can be gained by examining data from a high-spatial resolution sensor, e.g. the OPS instrument carried by the JERS-1 satellite. The OPS is a visible and shortwave infrared radiometer that makes radiance measurements in eight wavebands, each at a slightly higher spatial and spectral resolution than Landsat TM (Nishidai 1993). Figure 3 shows a daytime subscene of Lascar's active crater, recorded by the OPS instrument on 22 April 1993. Images from two channels are shown, with each pixel corresponding to a ground area of around 18 × 24 m. In both images the majority of pixels are recording solar radiation reflected by the crater and its surroundings. However, the 1.6-μm image contains a grouping of bright pixels at the centre of the active crater, which is a radiant anomaly corresponding to high-temperature areas of the lava dome (Denniss et al. 1996). Evidence that this is not simply an area of high surface reflectance comes from the lack of a corresponding anomaly in the 0.56-μm channel. This wavelength would show any surface reflectance variation, but is too short to be sensitive to thermal radiance from the hot surfaces. A 1- × 1-km box (the nominal size of the ATSR nadir-view measurements) has been overlaid on the 1.6-μm scene to illustrate the spatial resolution of the ATSR measurements. In reality, the crater is unlikely to be centred within a single ATSR measurement and may affect up to four neighbouring measurements, from which the relevant volcanic signal must be extracted.

The 1.6-μm sensor of ATSR-1 was uncalibrated prior to launch, but Wooster (1996) has shown that its response to incoming radiance is linear, and has calibrated the data so that accurate measurements of spectral radiance can be obtained. Our investigations have shown that, for the purposes of this study, the response of the channel has not varied significantly since launch, though the background noise level does vary a little between each scene. ATSR-2 incorporates an onboard calibration mechanism for the 1.6-μm waveband that allows continuous monitoring and calibration of the

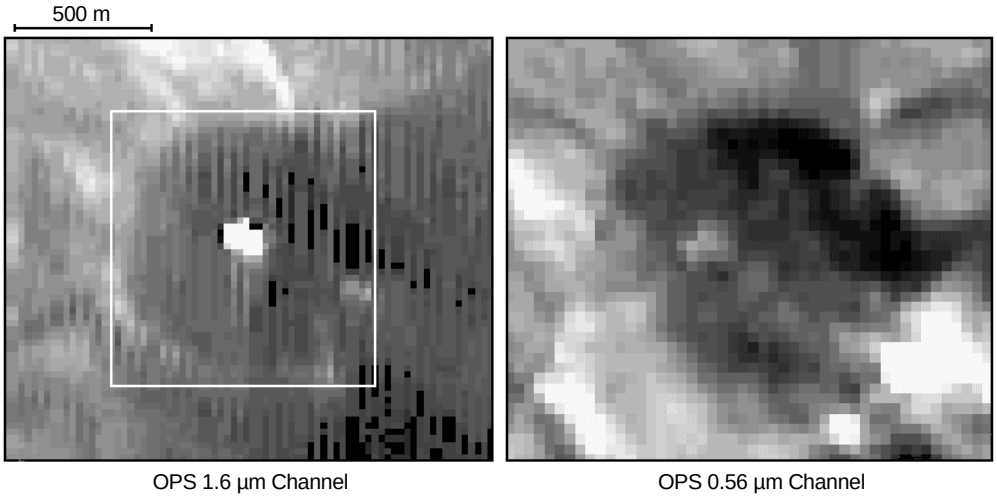

Fig. 3 A daytime subscene of Lascar's active crater, taken by the JERS-1 OPS instrument on 22 April 1993. The bright grouping of pixels in the 1.6-μm image, not evident at 0.56 μm, corresponds to an area of high-temperature thermal emittance associated with the lava dome. A 1- × 1-km box is overlain on the 1.6-μm image to indicate the nominal size of the ATSR nadir view radiance measurements

channel response (Read et al. 1992). Both ATSR instruments incorporate a sensitive calibration and recording mechanism for the longer wavelength infrared wavebands, allowing infrared brightness temperatures to be measured to accuracies of around 0.05 K (Delderfield et al. 1985; Smith et al. 1994).

Thermal emittance at 1.6 and 11 μm

The emissivity of andesitic lava, such as that comprising Lascar's dome, is greater than 85% in each of the ATSRs three thermal infrared wavebands (Salisbury and D'Aria 1994). Our measurements, made using a visible and shortwave infrared spectrometer and the techniques outlined in Salisbury and D'Aria (1992), show that the emissivity of andesite at 1.6 μm is greater than 92%. The lava dome is thus expected to be an efficient emitter of infrared radiation throughout the spectral region of interest, as are most rocks.

Reports of Lascar's summit activity (e.g. Smithsonian Institution 1992a) and examination of high-spatial-resolution imagery (Fig 3) indicate that during daytime observations any thermal signal present in ATSRs 1.6-μm channel is likely to be dominated by solar reflected radiation. We therefore use nighttime data, thus ensuring that all radiance measurements relate directly to elevated surface temperatures, in accordance with the Planck function (Eq. (1)):

$$L_\lambda(T) = \frac{C_1}{\pi\lambda^5\left(\exp\left(\frac{c_2}{\lambda T}\right)-1\right)} \quad (1)$$

where λ = wavelength (μm), T = temperature (K), L = spectral radiance (W/m^2/sr per micron), and C_1 and C_2 are constants (3.74×10^8 Wm^2 and 1.44×10^4 mK, respectively).

Over any particular temperature range, Eq. (1) can be approximated by a simple non-linear function of the type shown in Eq. (2):

$$L_\lambda(T) = aT^b, \quad (2)$$

where a and b are constants dependent upon the temperature range chosen.

Over the range of geothermal temperatures expected (~300–1000 °C), the 1.6-μm radiance ($L_{1.6}$) is approximately proportional to the tenth power of the temperature (Fig. 4). Thus, the levels of SWIR 1.6-μm radiance emitted from the hottest parts of the lava dome surface will be high and should be detectable by ATSR even if, as expected, these hottest areas only fill a very small fraction of the sensor's 1-km^2 field of view. Figure 4 also indicates that even relatively small amounts of cooling in these hottest areas will lead to a significant fall in emitted 1.6 μm radiance; thus, such changes should also be detectable by ATSR. The relatively small amounts of 1.6 μm radiance emitted by surfaces much below 200 °C are undetectable by ATSR; thus, the 1.6-μm signal is unaffected by variations in the low-temperature areas of the dome surface or in the still colder ambient background. Provided that the broad surface temperature of the lava dome does not rise significantly above the 100–200 °C level recorded by Oppenheimer et al. (1993), the radiances recorded in the ATSR 1.6-μm channel will relate directly to the surface area and temperature of material visible to the sensor that is heated magmatically or by magmatically driven fumaroles.

Over the 300–1000 °C temperature range, the thermal radiance emitted at 11 μm varies only with the square of temperature (Fig. 4). The 11-μm signal recorded by ATSR will therefore be dominated by surfaces presenting large areas to the sensor, principally broad areas of the lava dome and the ambient background. If the highest-temperature areas are of the relatively small sizes observed by Oppenheimer et al. (1993), then these surfaces will make relatively little contribution to the overall 11-μm signal.

In the same temperature range, the radiant emittance at 3.7 μm is proportional to T^4. However, recording of the 1.6- and 3.7-μm signals on ATSR-1 is mutually exclusive and 3.7-μm data of Lascar's hot spot are only available in the ATSR-2 scenes.

Methodology

Dataset

We examined 96 ascending-node (nighttime) scenes selected from the ATSR data archive held at the Ruther-

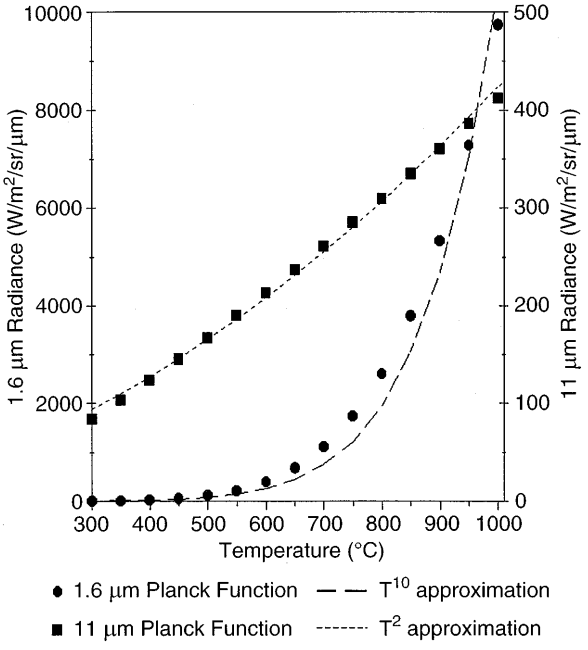

Fig. 4 The relationship between emitted radiance and brightness temperature for the ATSR 1.6- and 11-μm channels, calculated using the Planck function (Eq. (1)). The dashed lines show the relationships obtained if the Planck function is approximated by Eq. (2)

ford Appleton Laboratory, UK, and recorded between April 1992 and December 1995. Each scene covers a 512- × 512-km region containing the site of Lascar Volcano, and the data volume exceeds two scenes per month, potentially providing information at a temporal frequency close to the minimum degassing time scale recognised by Matthews et al. (1997). The majority of our data are from ATSR-1, with a small number of 1995 ATSR-2 scenes. Our ATSR time series overlaps the Landsat TM time series, allowing comparison of the high- and low-spatial-resolution datasets.

Data extraction

Because of the unusual scanning geometry of the ATSR sensor (Fig. 2), geocoding of data products is performed by the ATSR data processing system developed by the Rutherford Appleton Laboratory (Zavody et al. 1994). This procedure tags each ATSR measurement of radiance with a latitude/longitude location, which is intended to facilitate location of geographical areas within the scene. However, ATSR data processing is geared towards the retrieval of sea-surface temperature; thus, the geocoding procedure assumes that each pixel is at sea level. This causes significant geolocation errors over high-elevation targets such as Andean volcanoes. Our trigonometric calculations show that the error in geolocation due to Lascar's 5600-m altitude should be a maximum of 0°02' (ca. 2 km) in the nadir view and 0°05' in the forward view, the exact value being dependent upon the location of the volcano within the ATSR scan. To locate Lascar accurately within each ATSR scene we designed an automated software routine that pre-selects a 0°05' area of latitude and longitude, centred on the true latitude/longitude of the volcano, and then searches for the highest 1.6 μm signal in both the nadir- and forward-view data. The selected locations are then taken to be the actual site of Lascar, there being no other likely major high-temperature sources in the vicinity of Lascar. The signal in each of the available wavebands was then extracted for a 5 × 5 pixel grid centred on this location, allowing the local ambient background emittance in each thermal waveband to be quantified. The noise statistics for the 1.6-μm channel are computed using a larger 50 × 50 pixel area. Using this technique, data from all 96 scenes can be extracted within a few minutes.

Figure 5 shows a plot of the 1.6-μm data for a 20 × 20 pixel area of a nadir-viewing ATSR-1 scene recorded at 01:36 GMT on 29 September 1992. High-temperature surfaces within the active crater have caused the 1.6-μm signal to become elevated above the noise that characterises the remainder of the subscene. In this case the summit activity has affected two ATSR pixels, this being a function of the area covered by the lava dome and the exact geographical location and overlap of the ATSR measurements. In accordance with the technique of Oppenheimer et al. (1993), we used the

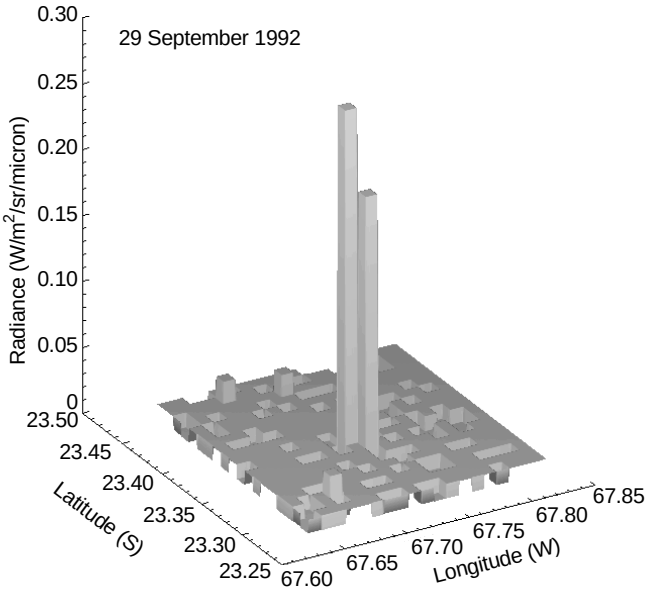

Fig. 5 A subset of the nighttime 1.6-μm nadir-view data recorded by ATSR at 01:36 GMT on 29 September 1992. In the absence of solar radiation the majority of the pixels are characterised by detector noise but, at the location of Lascar Volcano, a strong 1.6 μm signal is present

total "volcanic" signal in our analysis, obtained by summing the anomalous radiance of all pixels more than 2 σ above the background noise level. Since each radiance measurement recorded by ATSR is constructed by integrating the received signal for a finite period of time (75 μs), summing the signal from neighbouring pixels is equivalent to increasing this integration period and thus is consistent with the physical principles of the instrument. We note that the trend in this summed value followed that of the most affected pixel.

Cloud detection

The presence of cloud over the active crater will affect the signals in all the ATSR wavebands. It was therefore vital for us to identify data that were affected by cloud if the temporal analyses were to be solely representative of changes in the volcano's summit activity. Where large cold cloud bodies occurred over Lascar, anomalously low 11-μm brightness temperatures, approximately 10 K below the 257–272 K temperature range that characterised a cloud-free crater, were recorded. Data that showed 11-μm brightness temperatures below 250 K were therefore rejected from the study. This first-order cloud test eliminated 27 scenes, indicating that cloud obscuration is a significant factor even at Lascar, which is likely to be less affected by cloud cover than most other volcanoes since it resides in a region characterised by low rainfall.

Clouds smaller than a pixel (subpixel clouds) were more difficult to detect but, since such clouds could

possibly mask from view any thermal anomalies in the active crater, it was important to detect the instances in which they occurred. Additionally, the volcanic plume from Lascar could itself mask the surface. A standard method of subpixel cloud detection for AVHRR data is to analyse the variation in 11-μm brightness temperature within a 3×3 pixel grid. If this variation is greater than a pre-determined threshold, then the area is flagged as cloudy (Saunders 1986). The widely varying elevation and ambient temperature of land surfaces around Lascar, and the presence of thermal anomalies in the crater, prevented this test from being applied successfully. Therefore, we developed a new subpixel cloud test, specific to the conditions present at Lascar Volcano.

The principal characteristics of Lascar in the remaining 69-scene dataset were an 11-μm brightness temperature greater than that of the immediately neighbouring pixels and a 1.6-μm signal elevated more than 2σ above the background noise level. Five scenes lacked an elevated brightness temperature in both channels and these scenes were rejected from the study. We were confident that in these cases the ATSR was not viewing the hot surfaces within the active crater, probably because of complete obscuration by subpixel cloud or plume.

In three scenes an anomaly existed at 11 μm but not at 1.6 μm. A likely explanation of this is a decrease in the temperature of the lava dome surface, below which detectable amounts of 1.6 μm radiance are emitted. These scenes were therefore retained in the study. However, since the 1.6-μm signal is more affected by scattering from water droplets than the 11-μm signal (Zavody et al. 1994), this situation could also arise if small amounts of plume were present in the crater.

In two scenes an anomaly existed at 1.6 μm but not at 11 μm. The sensitivity of 1.6-μm radiance to scattering processes suggests that radiance from the lava dome was not being significantly scattered by clouds or plume; thus, these scenes were also retained. The low 11-μm measurements may be attributable to the presence of a high-level subpixel cirrus cloud within the ATSR field of view containing the active crater. The presence of such a subpixel cloud would lower the recorded 11-μm brightness temperature but, provided the hottest surfaces of the lava dome remained unobscured, would leave the 1.6-μm signal relatively unaffected.

A total of 64 "cloud-free" scenes survived our tests, spanning the period 7 April 1992–6 December 1995.

Non-volcanic sources of variability

Sensor viewing geometry Throughout this study, in the nadir-view data the zenith angle to Lascar was $12 \pm 5°$. We calculate that this viewing geometry is sufficiently near vertical that the whole of the dome would have been in view (unshielded by the crater walls) in each image. This is not the case for the forward-view data, taken at 55° from zenith, and (as expected) in most cases no forward-view 1.6-μm signal is evident. We have therefore concentrated on information contained within the nadir-view scenes.

Researchers intending to use MODIS data for similar studies should note that towards the scan edges, MODIS will have a viewing geometry comparable to that of the ATSR forward view. This suggests that only data from the near-nadir portion of the MODIS scan will be reliable for documenting activity within deep volcanic craters.

Atmospheric absorption Before interpreting the nadir-view data, it was important to quantify the amount of SWIR variation that could be due solely to variations in atmospheric transmission. The high elevation of Lascar means that its summit lies well above the bulk of Earth's atmospheric water vapour, and therefore above the main region of infrared absorption. Nevertheless, some atmospheric absorption of the radiation emitted from the summit region is inevitable and we allowed for this using the LOWTRAN 7 radiative transfer routine (Kneizys et al. 1988). Summer and winter atmospheric profiles for Lascar's latitude and elevation (Houghton 1986) were used with LOWTRAN to determine the atmospheric transmission over each of the ATSR channels and for each of the viewing geometries used. Assuming a standard concentration of tropospheric aerosols, transmissivity varied between 0.97 and 0.98, 0.94 and 0.96, and 0.96 and 0.97 for the 1.6-μm, 3.7-μm and 11-μm channels, respectively. This absorption will be countered by a small but variable amount of atmospheric emittance within the 11- and 3.7-μm wavebands, and a small amount of path radiance due to scatter in the 1.6-μm band. Thus, the atmospherically induced variability in the received radiances is low; a few percent at most for the 1.6-μm channel. Our analysis does not allow for the variable effects of volcanogenic aerosols and gases within the active crater. However, when we compare ATSR 1.6-μm measurements made only a few days apart, we see very few outliers of the sort that we would expect if these were major factors.

Results

The area and temperature of the lava dome surface

Figure 6a shows the 1992–1993 time series of ATSR 1.6-μm measurements. The 1992 lava dome that is responsible for this varying 1.6-μm signal was first seen during an overflight in March 1992. Photographs taken at that time indicate that the area occupied by the lava dome was approximately 2.5% of the ATSR 1-km^2 field of view, with the remainder being ambient background (Smithsonian Institution 1992a). Adapting the relations derived by Dozier (1981) and Rothery et al. (1988), Eq. (3) can be used to predict the radiance (R_i)

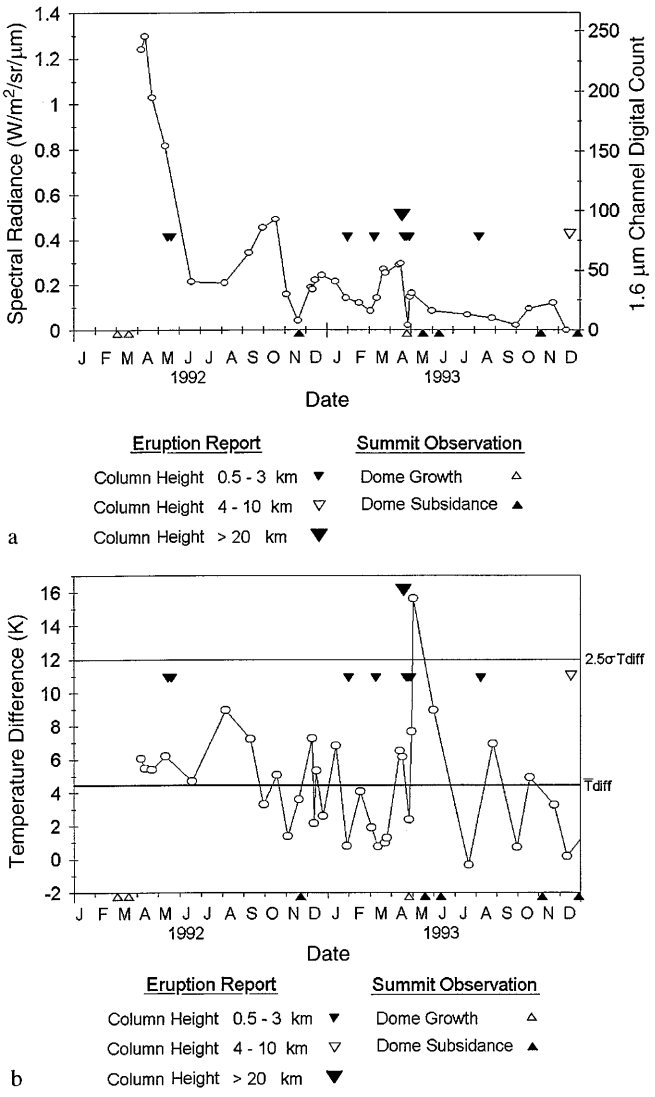

Fig. 6a The volcanogenic radiant flux detected in the 1.6-μm channel of ATSR-1 for the years 1992 and 1993. All measurements are nadir viewing and recorded in the absence of solar radiation (01:20–01:50 GMT) **b** The brightness temperature difference between the Lascar "summit" pixel and its immediate neighbours, recorded in the nadir-viewing 11-μm channel of ATSR over the years 1992 and 1993. The mean and 2.5-σ levels are also shown and all measurements are taken between 01:20 and 01:50 GMT. The hot pyroclastic flow, produced during the eruption of 20 April 1993 (Fig. 9), caused the 11-μm anomaly to rise above the mean +2.5-σ level

that would have been recorded in each of the ATSR wavebands if the ATSR field of view contained a lava dome having n different temperature components:

$$R_i = {}_i\tau_i \sum_{k=1}^{n} P_k L_i(T_k) + Ra_i^{\uparrow} + (1 - {}_i) Ra_i^{\downarrow} + Rb_i \qquad (3)$$

Where R_i is the radiance recorded in the ATSR channel having central wavelength i μm (W/m^2/sr per micron)
$L_i(T)$ is the Planck function for wavelength i
T_k is the surface temperature of the kth temperature component (K)
P_k is the fraction of the ATSR field of view covered by the kth temperature component of the lava dome
$_i$ is the emissivity of the surface at wavelength i
τ_i is the atmospheric transmission at wavelength i
$Ra_i^{\uparrow}$ is the upwelling atmospheric radiation at wavelength i, (W/m^2/sr per micron)
$Ra_i^{\downarrow}$ is the downwelling atmospheric radiation at wavelength i (W/m^2/sr per micron)
Rb_i is the radiance at wavelength i emitted by the ambient background contained within the field of view (W/m^2/sr per micron). Rb_i is zero for the 1.6-μm channel

As indicated previously, the emissivity of the dome and surrounding surfaces is known to an adequate precision, and the atmospheric parameters are estimable using LOWTRAN 7. By rearranging Eq. (3) and incorporating the Smithsonian Institution (1992) value for dome area, we used the recorded values of 1.6- and 11-μm radiance to determine the different thermal components of the lava dome surface. Since ATSR provides data in two distinct wavebands, Eq. (3) may be solved for $n=1$ or $n=2$, i.e. the lava dome having one or two distinct thermal components. Rothery et al. (1988), Glaze et al. (1989a) and Oppenheimer et al. (1993) all assume this thermal distribution when analysing Landsat TM data of Lascar, and Oppenheimer et al. (1993) have validated the assumption with field measurements of the post-February 1990 dome.

Using the 1.6-μm radiance level of 1.3 W/m^2/sr per micron, recorded at the start of April 1992, Eq. (3) provides results that are consistent with either of two end-member models: (a) the whole-dome surface area being a single temperature component of around 425 ± 25 °C, or (b) the dome being composed of two distinct temperature components, small areas (0.2–2% of the dome surface) at magmatic temperatures of 700–1000 °C, with the remaining majority area at a temperature too low to emit detectable radiance at 1.6 μm (i.e. < 200 °C).

An indication of the actual situation was gained by analysing the 11-μm brightness temperature difference between the "summit" pixel and its immediate neighbours. Throughout April, May and June 1992 the summit exhibited an almost constant 5.5 ± 0.5 K anomaly in the 11-μm brightness temperature data (Fig. 6b). If end-member model (a) were true, Eq. (3) indicates that an 11-μm brightness temperature anomaly of around 25–30 K would have been recorded, clearly much larger than that observed. We therefore conclude that the more appropriate model is that of end-member (b), with small fractions of the dome at near-magmatic temperatures and the broad area at a relatively low temperature. We can estimate the temperature of this broad area by assuming that the remainder of the ATSR field of view was occupied by surfaces at the ambient background temperature of –7.5 °C, this value being taken from the 11-μm measurements neighbouring the summit crater. Taking into account the relatively

minor 11-μm signal supplied by the very small high-temperature fractions, the broad area of the dome had a surface temperature of 90–130 °C (Eq. (3)). This is within the range of field measurements reported by Oppenheimer et al. (1993). Changes in the 1.6-μm signal should therefore be independent of low-temperature variations in the broad area of the dome surface, and this result validates our methodology for detecting change in the high-temperature areas using radiances measured at 1.6 μm.

April 1992–April 1993

The complete set of ATSR 1992–1995 nadir-view 1.6-μm observations is plotted, together with the TM 1.6-μm time-series data, in Fig. 1. The difference in the TM and ATSR spatial resolutions makes the magnitude of the radiances detected by each sensor widely different. To facilitate comparison, we have scaled the vertical axes to equalise the peak values of radiance recorded by each sensor. Significantly, we find that the observed drop in radiance between the final two Landsat TM scenes (15 April 1992 and 24 February 1993) is confirmed by data from 18 ATSR scenes covering the same period. This indicates that the ATSR is providing data of a similar quantitative value to Landsat TM, but at a temporal interval that allows major SWIR radiance variations to be confirmed by a time-history of measurements.

The TM data of Fig. 1 indicate that the 1.6-μm radiance had dropped to 30% of its 15 April 1992 value by 24 February 1993. This is really a minimum estimate of the radiance decrease, because a large proportion of the April 1992 TM pixels are saturated and provide only a lower limit on the amount of radiance arriving at the sensor. ATSR suggests a larger decline in radiance over this period and, since these measurements are unsaturated, this is believed to be a more reliable guide to the scale of the change.

Figure 6a shows the 1992–1993 ATSR 1.6-μm time series in more detail, with information from all available field reports overlain. The unsaturated ATSR data actually demonstrate a 90% decrease in radiance over the April 1992 -February 1993 period, with the major change occurring between April and June 1992. This rapid 3-month fall indicates that the size or temperature (or both) of the hottest areas decreased considerably. A possible mechanism for this change is subsidence of the lava dome, blocking the passage of hot magmatic gases through the dome structure. However, it was not until November 1992 that the summit was visited and subsidence of the dome was actually reported (M. C. Gardeweg et al., unpublished data). This is 6 months after the ATSR radiance data indicate a significant change in the summit condition. Further evidence for a link between subsidence, gas flow/pressure and cooling may be provided by the small eruptions of 15 and 21 May 1992 (Fig. 6a), since these events may indicate an attempt to relieve rising internal gas pressure within the volcano.

After the steep April–May 1992 decrease in SWIR signal, the ATSR data indicate fluctuating levels of 1.6-μm radiance until the major April 1993 eruption. The period of these fluctuations is around 90–120 days and they suggest regular low-frequency changes in the highest temperature summit conditions, possibly related to periodic fluctuations in degassing. The relatively smoothly varying 1.6-μm signal contrasts with the widely fluctuating 11-μm measurements made over the same period (Fig. 6b). The variability of the 11-μm anomaly is due in part to variations in the area and temperature of the ambient background contained within the summit pixel. Variations in these parameters, which do not affect the 1.6-μm signal, make it difficult to isolate the 11-μm signal component relating to physical changes within the summit crater. Although the 11-μm data are of limited use, they do reveal a decreasing trend over the April 1992–April 1993 period suggesting that the broad surface of the dome was cooling throughout this time.

The April 1993 eruption

18 April 1993 marks the beginning of the largest historical eruption of Lascar Volcano and the 1.6-μm data recorded around this event are shown in more detail in Fig. 7. This eruption coincided with a small local maximum in the 1.6-μm radiance, which had been oscillating since the major decrease of April-June 1992 (Fig. 6a). The activity was characterised by pyroclastic flows and eruption columns extending up to 25 km altitude. In the few weeks immediately prior to the April 1993 eruption, ATSR provides no evidence of a significant change in state of the volcano. Instead, we point to the

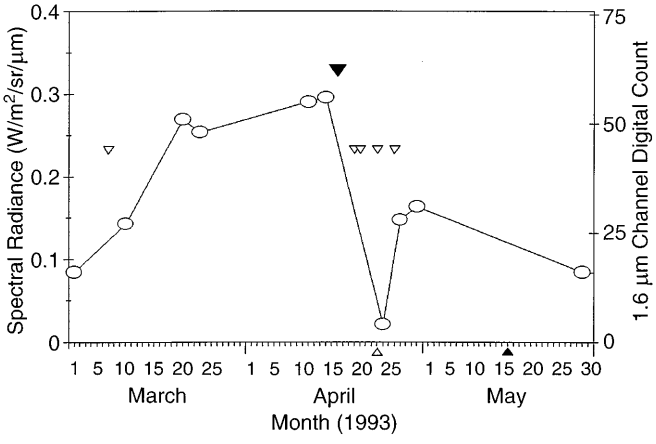

Fig. 7 The volcanogenic radiant flux detected in the 1.6-μm channel of ATSR-1 for the period surrounding the April 1993 eruption, the largest in the recorded history of Lascar Volcano. All measurements are nadir viewing and recorded in the absence of solar radiation (01:20–01:50 GMT)

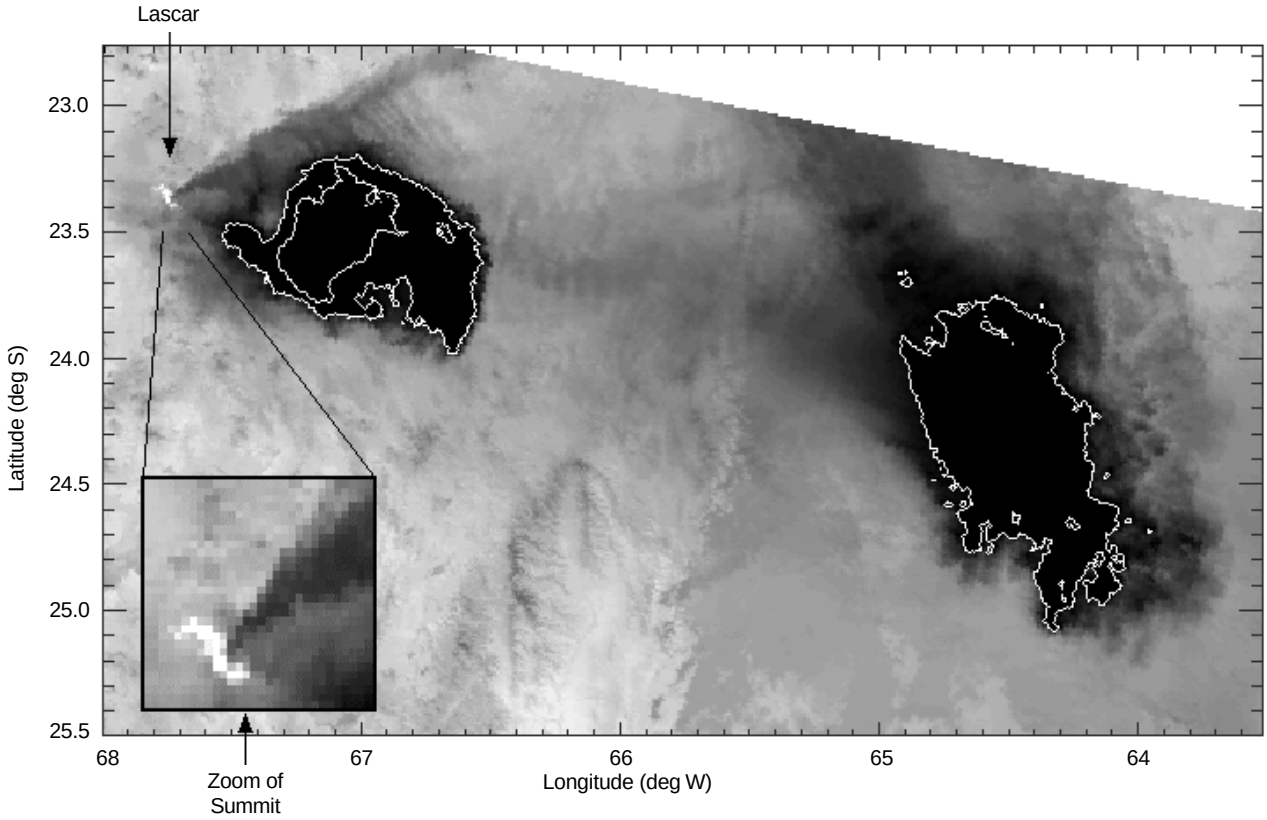

Fig. 8 The daytime ATSR 11-μm nadir-view scene recorded at 13:40 GMT on 20 April 1993, the date of the largest historical eruption of Lascar Volcano. This image clearly shows the two eruption columns produced on the morning of that day, with the –70 and –50 °C contours overlaid. The enlarged *inset* shows the recently emplaced pyroclastic flow deposit which saturated the 11-μm channel measurements

scale of SWIR radiance decrease between April 1992 and April 1993 as evidence of significant pre-eruptive changes occurring over a longer time scale. If the rapid April–June 1992 decrease in 1.6-μm radiance is due to a restriction in magmatic gas flow, then the restriction appears to have remained in place until the April 1993 eruption. This may indicate that the internal pressure of the volcano was increasing for the 10-month period since June 1992, and this long duration may be partly responsible for the anomalously large magnitude of the eruption.

Figure 8 reproduces the daytime ATSR 11-μm scene recorded at 13:40 GMT on 20 April 1993. This image clearly shows the two eruption columns produced that morning. At the time of the ERS-1 overpass the initial column, which was reported to have an altitude >15 km, had drifted 400 km NE of Lascar and had a minimum cloud top temperature of –68 °C. The second column, formed just 20 min before the image was acquired, was reported to have reached a slightly lower altitude (Smithsonian Institution 1993a) but possessed a colder cloud top temperature of –80 °C. We presume that this discrepancy is due to the effects of undercooling on the second plume (Woods et al. 1995). The earlier plume is likely to have equilibrated to the ambient air temperature and may also have had time to retreat to its neutral buoyancy height by the time this image was recorded (Woods and Kienle 1994).

Partial collapse of the second eruption column produced the farthest-reaching pyroclastic flows, travelling 7.5 km NW of the volcano. These are clearly visible in the magnified inset in Fig. 8. Pyroclast surface temperatures cannot be accurately determined since, at this short time after emplacement, the hot surfaces cause the 11-μm waveband to reach its 320 K saturation limit. However, it is simple to differentiate the pyroclastic deposits from active lava in the ATSR data. The former do not have surface material at or near magmatic temperatures and therefore do not show a thermal signal in the 1.6-μm channel.

Figure 6b shows that the emplacement of the pyroclastic flow was the only event associated with a significant rise in the 11-μm brightness temperature anomaly, above the 2.5-σ level. We suggest, therefore, that routine monitoring of the 11-μm anomaly could provide a method of detecting pyroclastic flow emplacement at this and other remote volcanoes.

April 1993–April 1994

Lascar's eruptive activity began to subside after 20 April 1993. Observers reported generally weak columns, barely rising above the crater rim, and small ex-

plosions on 22, 23, 26 and 29 April, whose incidence is indicated in Fig. 7. The ATSR data recorded on 28 April show minimal 1.6-μm radiance from the active crater, though aerial photographs taken on the 26 April show a new lava body occupying a much larger portion of the crater than did the previous dome. The new lava dome was around 380 m in diameter and 120 m thick, three times thicker than the previous dome structure (Smithsonian Institution 1993b). The dome was reported to have grown in less than 40 h between 24 and 26 April and contained a funnel-shaped indentation, possibly a result of the 26 April explosion (Smithsonian Institution 1993c). Since a new lava dome was present in the crater at the time, which we would expect to emit some SWIR radiance, it seems probable that the ongoing eruptive activity and plume-filled nature of the crater was responsible for the low 1.6-μm signal recorded on 28 April. The explosion on 29 April may have damaged the structure of the dome still further, but ATSR data recorded on 30 April and 3 May, after explosive activity had ceased, show that a substantial 1.6-μm signal had been re-established. This indicates the presence of a high-temperature thermal anomaly, but the signal level amounted to only a tenth of the maximum spectral radiance produced by the smaller 1991–1992 dome.

Aerial observations on 19 May indicated that the dome had started to subside and the increasing subsidence is tracked by a regular decrease in 1.6-μm radiance, reaching a local minimum on 30 September 1993 (Fig. 6a). An eruption is reported to have occurred sometime in August 1993, probably a result of the continuing dome collapse (Smithsonian Institution 1994a). By 5 November, observations made from the crater rim indicated that the collapsed area had reached a depth of 50–100 m below the surface of the dome (Smithsonian Institution 1993b). However, the increase in 1.6-μm radiance observed during October and November indicates that high-temperature thermal activity may have been intensifying, though the absolute magnitude of the radiances remained low. This contradicts the observations of April–June 1992, when dome subsidence was paralleled by a sharp fall in 1.6-μm signal, and suggests that an alternative mechanism was operating. The post-April 1993 lava dome is estimated to be three times thicker than the previous lava body (Smithsonian Institution 1993b), and it is possible that the thickness of this dome structure made it difficult for hot gases to escape from below. Ground observations and certain of the Landsat TM data suggest that when dome deflation occurs limited degassing continues from fumaroles on the crater floor (Oppenheimer et al. 1993; Smithsonian Institution 1992b, 1993b). We suggest that these fumarolically heated areas may be the source of much of the SWIR radiance seen in October–November 1993. The relatively low levels of 1.6-μm signal, compared with those seen in April 1992, may also indicate a change in SWIR radiance source. On 12 December the SWIR signal fell to zero, indicating that, whatever the source, degassing within the crater had most likely become restricted. Five days later, two large explosive eruptions occurred that produced columns rising up to 8 km above the summit. The fall in SWIR radiance may be linked to this subsequent eruptive event, although the magnitude of both phenomena was much smaller than those occurring between April 1992 and April 1993.

No ATSR observations exist for 4 months after the December eruption since, during this period, ERS-1 underwent a temporary orbit shift and was unable to image Lascar Volcano. However, a report of a summit visit on 19 February 1994 indicates that the post-April 1993 dome, and surrounding areas of the crater floor, had almost completely subsided into a deep hole centred on the active vent. Certain fumarole temperatures neighbouring this area were observed to be $>230\,^{\circ}C$, and there were warnings that another eruption was expected in the near future (Smithsonian Institution 1994a). These warnings were made on the grounds that degassing was constrained by large-scale subsidence of the system through which gas flow was previously channelled. These conditions were believed to be similar to those observed in previous eruptive cycles (Smithsonian Institution 1994a). However, for the next 5 months no explosive activity was reported by local observers, indicating that the internal pressure inside the volcano may have risen throughout this period.

April 1994–July 1995

In 1994–1995 only two reported visits were made to the volcano. Thus, remote monitoring of the emitted SWIR radiance provides information on otherwise undocumented changes. After the SWIR radiance minimum immediately before the December 1993 eruption, the recorded signal is seen to rise in consecutive measurements recorded in April, May and June 1994 (Fig. 9a). The SWIR radiance dropped at the start of July 1994, just prior to a period of renewed vulcanian activity that generated plumes rising 4 km above the crater. The SWIR radiance remained low during this event, probably because of scattering by plumes, and then rose until mid-September, fell slightly in October and peaked at the beginning of November. Small phreatic eruptions occurred between 13 and 19 November 1994, causing eruption plumes up to 3 km high (Smithsonian Institution 1994b). The SWIR signal lowered during these events but, since it returned to pre-November levels after the cessation of activity, we believe the lowering may again have been related to radiance scattering by eruption products. A summit visit in late November 1994 showed that the central hole in the crater floor had deepened and no lava dome was present (Smithsonian Institution 1995a). Again, the most likely interpretation for the 1.6-μm signal is radiance from fumarolically heated surfaces away from the subsidence

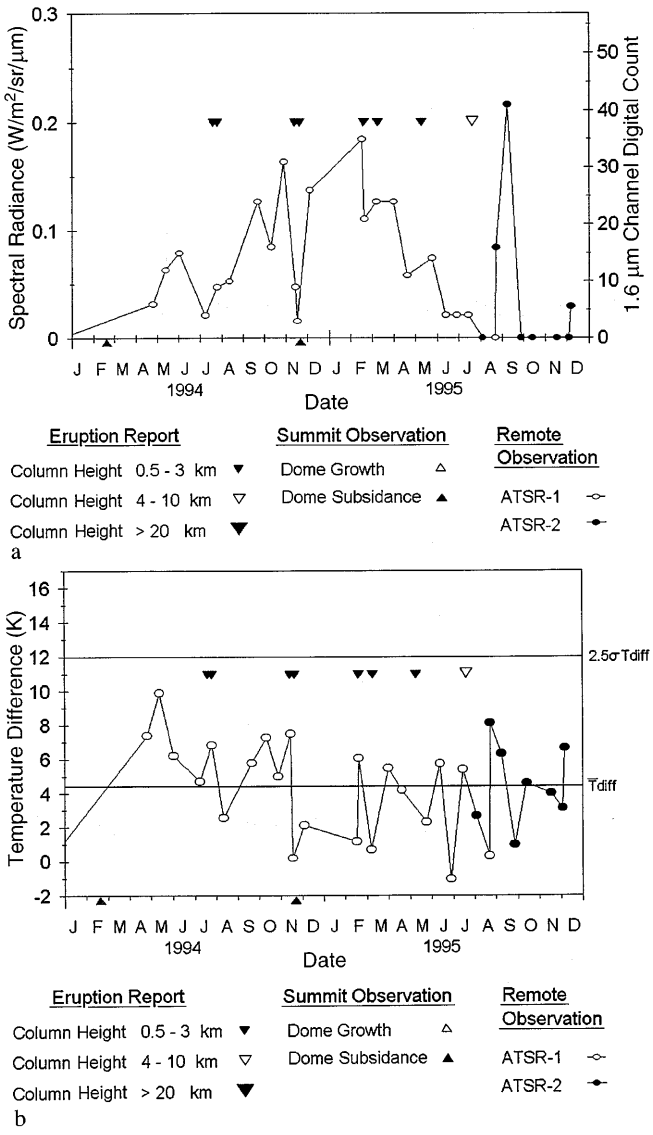

Fig. 9a The volcanogenic radiant flux detected in the 1.6-μm waveband of ATSR-1 (clear data points) and ATSR-2 (opaque data points) for the years 1994 and 1995. All measurements are nadir viewing and recorded in the absence of solar radiation (01:20–01:50 GMT). Note the expanded vertical scale as compared with Fig. 6a. **b**The brightness temperature difference between the Lascar "summit" pixel and its immediate neighbours, recorded in the 11-μm channel of ATSR over the years 1993 through 1995. All measurements are nadir viewing and recorded at night (01:20–01:50 GMT). The mean and 2.5-σ levels are also shown

area. Even when it had recovered from the November 1994 minimum, the magnitude of the 1.6-μm radiances remained much lower than the maximum levels recorded in April 1992.

The SWIR signal remained at a relatively constant level until February–March 1995, when a general decline in the radiance began. This may indicate the onset of decreasing gas flux through the crater floor fumaroles. There were small ash eruptions between 18 February and 10 March and three small explosive eruptions on 10 May 1995 (Smithsonian Institution 1995a). The SWIR radiance reached very low levels in June and mid-July, and these data suggest that the eruptions did not allow an increase in the subsequent rate of degassing, and in consequence surface temperatures remained low. If this mechanism is correct, then the general decline in radiance since February–March 1995 would indicate that a buildup of gas pressure below the crater floor may have been proceeding for up to 6 months. As a possible consequence of this, 20 July saw at least one, possibly two, larger vulcanian events, with plumes reported at altitudes of 6–9 km (Smithsonian Institution 1995b).

As stated above, we prefer to interpret the 1994–1995 trends in 1.6-μm radiance as due to variations in degassing from crater floor fumaroles. However, we cannot rule out the alternative possibility that this represents another (otherwise undocumented) cycle of dome growth and collapse. If this were the case, then the late November 1994 field observation of a hole in the crater floor, which coincides with a brief dip in the 18-month rise and fall in 1.6-μm radiance, must again represent only a temporary situation, caused by the destruction of a dome in the preceding November eruptions. In this hypothesis a new dome would have regrown after November and then began to subside in February/March, causing the decreasing 1.6-μm radiance trend.

July 1995–December 1995

After the July 1995 eruption, recorded SWIR radiance dropped to zero and remained undetectably low until August and September, when data indicate renewed onset of high-temperature activity (Fig. 9a). These observations were made with the ATSR-2 instrument, and 3.7-μm measurements are available in addition to those at 1.6 μm. The 3.7-μm brightness temperatures for the two readings in August and September are 20 K above all other ATSR-2 3.7-μm data points, in one case the measurement reaching the 320 K saturation temperature. This coincident rise in 1.6- and 3.7-μm signals confirms that these data relate to a temporary increase in high-temperature summit activity which, as expected, we do not observe in the highly variable 11-μm signal (Fig. 9b). The 1.6- and 3.7-μm radiance fell again without any reported eruptions, and 1.6-μm radiance remained negligible until a small rise in our last observation, recorded on 6 December 1995. The most recent reported visit was made on 6 February 1996 (Matthews et al., 1997) when the 1993 dome was seen to have been completely absent, leaving a deep pit with four fumarolic jets around its rim. We suppose that variations in degassing through these jets was responsible for the rises in SWIR radiance seen in September and December 1995 although, in this case, these variations do not appear to have signified pre-eruptive events.

Conclusion

This study has shown that measurements of volcanogenic shortwave infrared (1.6 μm) flux can be made using low-spatial-resolution satellite-based instruments such as the ATSR. The nighttime 1.6-μm signal is derived exclusively from high-temperature areas, and thus is not affected by changes in the ambient temperature or in surfaces having temperatures much below 200 °C. The information can therefore be interpreted as relating to changes in the hottest surfaces on the volcano. Large explosive eruptions appear to be more likely when the 1.6-μm signal has fallen from a high to a low level. The 11-μm signal is less useful, since it is difficult to isolate the signal caused by changes in the hottest areas of the summit.

The low spatial resolution of the ATSR 1.6-μm measurements ensures that the sensor does not become saturated, whereas the high temporal resolution (gained at the expense of spatial detail) allows a more comprehensive dataset to be collected than is possible with Landsat TM. The closely spaced nature of the time series also assists in identifying temporary excursions in the data that are attributable to accumulations of volcanogenic gases, aerosols or plumes. New cloud detection tests, specific to the volcanic conditions encountered, allowed cloud-contaminated data to be removed from the analysis.

Our observations of 1992–1993 variations in 1.6-μm flux from Lascar are consistent with observations made using high-spatial-resolution data (Oppenheimer et al. 1993; Smithsonian Institution 1993a), and with field observations of dome growth and subsidence (M. C. Gardeweg et al., unpublished data). Such data can therefore assist predictions of eruptive behaviour deduced from the application of models of lava dome growth to this and other similar volcanoes. We suggest that the magnitude of the April 1993 eruption may be related to the long interval between the initial decrease in radiance and the major eruptive event. After the major eruption of April 1993, the 1.6-μm flux never regained its April 1992 levels, indicating that these levels were anomalously high for the 1992–1995 period. This may be due to the relative thinness of the 1992 lava dome.

In addition to the April 1992–April 1993 activity, we observed a cycle of increasing SWIR radiance during 1994, and decreasing radiance during the first half of 1995, for which more direct observations are lacking. We suggest that this cycle is related to variations in gas flow through fumaroles on the crater floor and we observe that these variations are followed by a major explosive event. However, we cannot discount the possibility that this cycle represents an otherwise unobserved cycle of dome growth and collapse. A briefer and lower amplitude cycle is observed between October and December 1993, and this is also followed by a relatively large eruption. Our most recent data confirm field observations that, by October 1995, Lascar had entered a phase characterised by weak degassing.

The analytical techniques developed during this study will be applicable to the monitoring of certain volcanic targets using SWIR data from the low-spatial-resolution MODIS sensor and the forthcoming advanced ATSR instrument, both due to be launched in the late 1990s. However, lack of information in the ATSR forward view indicates that care must be taken to ensure that only data having the appropriate viewing geometry (usually near nadir-viewing) is used in such studies.

Acknowledgements This study is a result of an NERC Earth Observation Programme Board studentship funded by NERC and the Natural Resources Institute (Wooster), and European Space Agency ERS project UK101 (Rothery and Wooster). It would scarcely have been possible without the generous cooperation of C. Mutlow, N. Houghton and colleagues at the Rutherford Appleton Laboratory. The JERS data in Fig. 2 were supplied to Rothery under the terms of JERS-1 verification project NASDA J-0107, and were partly processed by A. Denniss (Denniss et al. 1996). We are most grateful to S. Sparks and S. Matthews for their encouragement, to C. Oppenheimer for use of the TM time-series data and to the reviewers L. Glaze and V. Realmuto for their exceedingly helpful comments and suggestions.

References

Asrar G, Jon Dokken D (1993) EOS Reference Handbook, NASA Earth Science Support Office, Washington DC

Delderfield J, Llewellyn-Jones DT, Bernard R, Javel Y de, Williamson EJ, Mason I, Pick DR, Barton IJ (1985) The along track scanning radiometer (ATSR) for ERS1. Proc SPIE Instrument Optical Remote Sensing from Space 589:114–120

Denniss AH, Harris AJL, Carlton RW, Francis PW, Rothery DA (1996) The 1993 Lascar pyroclastic flow imaged by JERS-1. Int J Remote Sensing 17:1975–1980

Dozier J (1981) A method for the satellite identification of surface temperature fields of sub-pixel resolution. Remote Sensing Environment 11:221–229

Francis PW, Rothery DA (1987) Using the Landsat Thematic Mapper to detect and monitor active volcanoes: an example from Lascar volcano, northern Chile. Geology 15:614–617

Glaze L, Francis PW, Rothery DA (1989a) Measuring thermal budgets of active volcanoes by satellite remote sensing. Nature 338:144–146

Glaze LS, Francis PW, Self S, Rothery DA (1989b) The 16 September 1986 eruption of Lascar Volcano, north Chile: satellite investigations. Bull Volcanol 51:149–160

Harris AJL, Rothery DA (1995) Thermal monitoring of volcanoes using data from the AVHRR. Proc 21st Annual Conference of the Remote Sensing Society, University of Southampton, 11–14 September, pp 528–535

Harris AJL, Vaughan RA, Rothery DA (1995) Volcano detection and monitoring using AVHRR data: the Krafla eruption, 1984. Int J Remote Sensing 16:1001–1020

Holasek RE, Rose WI (1991) Anatomy of 1986 Augustine volcano eruptions as recorded by multispectral image processing of digital AVHRR weather satellite data. Bull Volcanol 53:420–435

Houghton JT (1986) The physics of atmospheres, 2nd edn. Cambridge University Press, Cambridge

Holdaway R (1993) UK instruments for mission to planet earth. Space Technol 13:561–567

Kneizys F, Shettle E, Abreu L, Chetwynd J, Anderson G, Gallery W, Selby J, Clough S (1988) Users' guide to LOWTRAN 7. Air Force Geophysics Laboratory, Environmental Research Paper 1010, Hanscom AFB, Massachusetts

Lillesand TM, Kiefer RW (1987) Remote sensing and image interpretation, 2nd edn. Wiley, New York
Matson M (1984) The 1992 El Chichón volcano eruptions: a satellite perspective. J Volcanol Geotherm Res 23:1–10
Matthews SJ, Gardeweg MC, Sparks RSJ (1997) The 1984 to 1996 cyclic activity of Lascar Volcano, northern Chile; cycles of dome growth, dome subsidence, degassing and explosive eruptions. Bull Volcanol (in prep.)
Mouginis-Mark P, Rowland S, Francis P, Friedman T, Garbeil H, Gradie J, Self S, Wilson L, Crisp J, Glaze L, Jones K, Kahle A, Pieri D, Zebker H, Kruger A, Walter L, Wood C, Rose W, Adams J, Wolff R (1991a) Analysis of active volcanoes from the Earth observing system. Remote Sensing Environment 36:1–12
Mouginis-Mark P, Rowland ST, Garbeil H, Flament P (1991b) AVHRR observations of the Kupaianaha eruption, Hawaii. EOS, Transactions of the American Geophysical Union, AGU 1991 Fall Meeting Program and Abstracts:562
Nishidai T (1993) Early results from 'Fuyo-1' Japan's Earth Resources Satellite (JERS-1). Int J Remote Sensing 14:1825–1833
Oppenheimer C, Francis PW, Rothery DA, Carlton RWT (1993) Infrared image analysis of volcanic thermal features: Lascar Volcano, Chile, 1984–1992. J Geophys Res 98:4269–4286
Prata AJ (1989) Observations of volcanic ash clouds in the 10–12 μm window using AVHRR/2 Data. Int J Remote Sensing 10:751–761
Read P, Hardie A, Magraw J, Taylor H, Jelly J (1992) A calibration system, using an opal diffuser, for the visual channels of the along track scanning radiometer, ATSR-2. Proc Institute of Physics Conference on Photoelectronic Image Devices, London, UK, September 1991 (London, IOP), pp 207–213
Rothery DA, Francis PW, Wood CA (1988) Volcano monitoring using short wavelength infrared data from satellites. J Geophys Res 93:7993–8008
Rothery DA, Borgia A, Carlton RW, Oppenheimer C (1992) The 1992 Etna lava flow imaged by Landsat TM. Int J Remote Sensing 13:2759–2763
Salisbury JW, D'Aria DM (1992) Emissivity of terrestrial materials in the 8–14 μm atmospheric window. Remote Sensing Environment 42:83–106
Salisbury JW, D'Aria DM (1994) Emissivity of terrestrial materials in the 3–5 μm atmospheric window. Remote Sensing Environment 47:345–361
Saunders RW (1986) An automated scheme for the removal of cloud contaminations from AVHRR radiances over western Europe. Int J Remote Sensing 7:867–886
Smith A, Saunders R, Zavody A (1994). The validation of ATSR using aircraft radiometer data over the tropical Atlantic. J Atmospheric Ocean Technol 11:789-800
Smithsonian Institution (1992a) Lascar. Bull Global Volcanism Network 17 (5):12–13
Smithsonian Institution (1992b) Lascar. Bull Global Volcanism Network 17 (6):10–11
Smithsonian Institution (1993a) Lascar. Bull Global Volcanism Network 18 (4):2-6
Smithsonian Institution (1993b) Lascar. Bull Global Volcanism Network 18 (11):11–12
Smithsonian Institution (1993c) Lascar. Bull Global Volcanism Network 18 (8):34
Smithsonian Institution (1994a) Lascar. Bull Global Volcanism Network 19 (3):7-8
Smithsonian Institution (1994b) Lascar. Bull Global Volcanism Network 19 (11):7
Smithsonian Institution (1995a) Lascar. Bull Global Volcanism Network 20 (3):14–15
Smithsonian Institution (1995b) Lascar. Bull Global Volcanism Network 20 (6):11–12
Wen S, Rose WI (1994) Retrieval of sizes and total masses of particles in volcanic clouds using AVHRR bands 4 and 5. J Geophys Res 99:5421–5431
Woods AW, Holasek RE, Self S (1995) Wind-driven dispersal of volcanic ash plumes and its control on the thermal structure of the plume-top. Bull Volcanol 57:283–292
Woods AW, Kienle J (1994) The dynamics and thermodynamics of volcanic clouds. J Volcanol Geotherm Res 62:273–299
Wooster MJ (1996) In-orbit calibration of the ATSR-1 1.6 μm channel using high-resolution data from the JERS-1 (Fuyo-1) optical sensor. Int J Remote Sensing 17:1069–1074
Zavody AM, Gorman MR, Lee DJ, Eccles D, Mutlow CT, Llewellyn-Jones DT (1994) The ATSR data processing scheme developed for the EODC. Int J Remote Sensing 15:827–843